Colloids and Surfaces A: Physicochemical and Engineering Aspects 630 (2021) 127608

Contents lists available at ScienceDirect

Colloids and Surfaces A: Physicochemical and Engineering Aspects

journal homepage: www.elsevier.com/locate/colsurfa

Modulating nanocellulose hydrogels and cryogels strength by crosslinking and blending

Laila Hossain, Vikram Singh Raghuwanshi, Joanne Tanner, Gil Garnier *

Bioresource Processing Research Institute of Australia (BioPRIA), Department of Chemical Engineering, Monash University, Clayton, Australia

HIGHLIGHTS

- Mechanical properties of crosslinked and blended nanocellulose gels were studied.
- Physical and chemical crosslinking significantly increases hydrogel strength.
- Cryogel strength is increased by CNC blending.
- Chemical crosslinking and CNC blending increase cryogel structure homogeneity.
- Cryogel liquid absorption capacity decreases with crosslinking or blending.

GRAPHICAL ABSTRACT

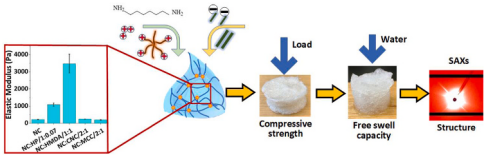

ARTICLE INFO

Keywords:
Mechanical strength
Nanocellulose
Hydrogel
Cryogel
Cellulose nanocrystal

ABSTRACT

The mechanical strength of hydrogels and cryogels made from carboxylated nanocellulose (NC) fibers can be modulated by chemically/physically crosslinking and blending with different fibrils (shorter/longer). Nanocellulose hydrogels are produced by oxidizing Bleached Eucalyptus Kraft (BEK) pulp followed by high pressure mechanical treatment. Polyethyleneimine (PEI) and hexamethylenediamine (HMDA) were selected to crosslink nanocellulose hydrogels physically and chemically, respectively. Shorter cellulose nanocrystals (CNC) and longer microcrystalline cellulose (MCC) fibrils were blended with the TEMPO oxidized nano/micro fibers to produce hydrogels of controlled properties. Nanocellulose cryogels were prepared from these hydrogels by a two steps process of freezing and lyophilization. The mechanical properties of nanocellulose hydrogels and cryogels were modulated by controlling the type and density of crosslinking as well as by blending with nano- or microfibrils. Chemical crosslinking (HMDA) increases the hydrogel elastic compression moduli (G′) but does not significantly affect the compressive strength of the cryogel. SAXS reveals the HMDA crosslinked hydrogel to be structurally homogeneous. Physical crosslinking with high molecular weight PEI increases the storage modulus (G′) of nanocellulose hydrogels. Blending a carboxylated nanocellulose fiber suspension with CNC significantly increases the cryogel compressive strength. Nanocellulose gel exhibits tuneable mechanical strength and absorption capacity from the crosslinking/blending strategy (type and density); this improved fundamental knowledge of the fiber-crosslinker and fiber-cellulose crystal interactions enables greater control and tunability of the properties of hydro- and cryogels for personal and infant care products, as agricultural water retention aids, and for biosensor applications.

* Corresponding author.
E-mail address: gil.garnier@monash.edu (G. Garnier).

https://doi.org/10.1016/j.colsurfa.2021.127608
Received 29 July 2021; Received in revised form 15 September 2021; Accepted 18 September 2021
Available online 22 September 2021

1. Introduction

A hydrogel is a three dimensional polymeric network capable of retaining a large volume of water inside its structure [1,2]. Such polymeric materials have wide-ranging applications as a wet or dried gel, including baby diapers, contact lenses, drug delivery, wound dressing, and tissue engineering, among others [3–7]. The term hydrogel is often used ambiguously to describe both the wet and dried gel forms, although the term "cryogel" describing freeze-dried gels provides clarity [8]. Collectively, hydro- and cryogels can be categorised as synthetic or naturally derived, depending on their raw material [9,10]. Synthetic hydrogels based on acrylate or acrylamide are the most commonly used for commercial applications, but they are neither renewable nor biodegradable. Common naturally derived hydrogels include alginate, chitosan, collagen, gelatine, starch, hyaluronan, and recently, cellulose [11,12]. Among those, cellulose-based materials are attractive because of their stiffness, hydrophilicity, ease of functionalization, renewability, biocompatibility, large availability and low cost, making them unique among biodegradable materials [13,14].

Cellulose is the most abundant biopolymer on Earth. It is found in plants, algae, tunicates and some bacteria [15,16]. Plant-derived cellulose (and nanocellulose) contains both crystalline and amorphous regions, depending on the local molecular structures [17]. Breaking down the cellulose can produce nanocellulose (NC) of three different types: (i) cellulose nanofiber (CNF), (ii) cellulose nanocrystal (CNC), and (iii) bacterial cellulose (BC). CNF is prepared either by (i) mechanical treatment, (ii) chemical treatment or (iii) combined chemical and mechanical treatment of plant-derived cellulose. CNF retains both the amorphous and crystalline regions of the original cellulose fibers [18]. CNC is mainly produced by acid hydrolysis of plant-derived cellulose fibers to degrade the amorphous regions and retain the crystalline domains [19]. Bacterial cellulose is produced by microorganisms that excrete pure cellulose directly as nanofibres. In general, nanocellulose is biocompatible and has excellent native gel forming properties [20].

The mechanical properties of a nanocellulose hydrogel govern many of its applications [21] in which crosslinking (type and density) can be a controlling variable. Crosslinking compounds can be broadly categorized as chemical or physical, depending on the type of interaction between the crosslinker and the nanocellulose fiber. Chemical crosslinkers form covalent bonds with nanocellulose fibers. Common examples include methylene-bis-acrylamide, ethylene glycol dimethacrylate (EGDMA), 1,1,1- trimethylolpropane triacrylate (TMPTA), and tetraallyloxy ethane (TAOE) [2,22]. Epichlorohydrin, hexamethylenediamine (HMDA), aldehydes and aldehyde-based reagents, urea derivatives, and carbodiimides have also been used as crosslinkers for cellulose based hydrogels [23,24]. Among these, crosslinking of nanocellulose fiber with high carbon amine groups in presence of EDC/sulfo NHS is very efficient with high yield [25].

In physical cross-linking, interacting forces such as hydrogen bonding, electrostatic forces, van der Waals forces, chain entanglements, and ionic and hydrophobic interactions dominate [26]. Physical cross-linking via hydrogen bonding between the carboxyl groups of oxidized cellulose fibers can be achieved by the freeze-thaw technique. The skeletal density of the cellulose fiber matrix is increased upon crystallization of the bulk solvent, which forces the polymer chains to align and form a cohesive network via hydrogen bonding and covalent interaction. Changes in the freeze-thaw cycle affect the resultant hydrogel properties, for example, reduction of porosity [27–29]. High strength polyvinyl alcohol (PVA) hydrogels have been made by this technique, where the strength came from intra and intermolecular hydrogen bonds [30]. The freeze-thaw method has also been used to make high strength hydrogels from hemicellulose, hyaluronic acid and cellulose nano crystal [31–33]. However, the freeze-thawing method has some disadvantages: (i) long cycle times (for example, five cycles or more with 22 h each) [34] (ii) irregular hydrogel pore spacing and (iii) higher energy consumption due to repeated cycles. Physical crosslinking can also be achieved by the physical interaction of cellulose fiber with positive polyelectrolyte molecules, resulting in high mechanical strength. For example, polyethyleneimine (PEI) has been widely used to crosslink with nanocellulose in the presence of glutaraldehyde [35]. Nanocellulose fibers crosslinked with PEI and allylamine modified PNIPAm particles have been developed and exhibit thermo-responsive behaviour [36]. As the definition of physical crosslinking includes hydrogen bonding and ionic/electrostatic interaction [37], the ionic interaction between positive PEI molecules and negative nanocellulose fibers can be designated as physical crosslinking. For a greener physical crosslinking approach, it may be possible to use PEI alone, although there is limited work on this. Therefore, the effect of PEI molecular weights on nanocellulose fibers crosslinking is also poorly understood.

Cryogels are hydrogels that have been dried into porous and highly absorbent structures with high surface area. Cryogels can be produced by supercritical drying, freeze drying, ambient pressure drying, microwave drying, or vacuum drying of hydrogels [38]. Cryogels have been investigated for multifunctional sensor, supercapacitor, insulator, controlled drug release and drug scaffold, and recently, infant care applications [8,39–43]. The absorption capacity of a cryogel is a critical parameter for all applications, and is related to its cross linking density, internal surface area, and charged functional groups, such as COO^- [44]. Oxidation is the most common treatment to introduce negative hydrophilic COO^- groups on the fiber surface [45,46]. The hydrophilic functional groups (COO^-) of the cryogel network contribute to water absorption while the cross-links between the network chains prevent the cryogel structure from collapsing upon re-wetting [47]. The mechanical/compressive strength of cryogel can also be increased upon cellulose crystal blending [48]. The chain molecules of crystalline cellulose are packed in an orderly manner resulting in higher nanocellulose strength compared to amorphous region [49]. Introducing nano and micro crystal into the nanocellulose cryogel affects the bonding surface area and the total fiber length available for binding.

In spite of their wide commercial use, there is surprisingly limited knowledge describing how physical and chemical crosslinking correlates with hydrogel and cryogel mechanical strength. For example, the change in mechanical strength for hydrogels and cryogels has not been correlated with their physical and chemical crosslinking density. In this study, HMDA is chosen as chemical crosslinker because HMDA is widely known and used due to its six carbon chains, which form chemical crosslinks between nanocellulose fibers more effectively than other low carbon amines. As physical crosslinker, we have used PEI alone to form ionic interaction with nanocellulose fibers while ensuring to avoid any hazardous chemical during gel preparation. Cellulose crystal was blended with nanocellulose fiber to go one step closer towards the sustainability. Blending cellulose crystal is potentially greener option as PEI and HMDA are still chemical additives and removal of this additives can make the cryogel even greener and sustainable. The effect of cellulose crystals blending has also not been investigated or quantified. In addition, the absorption capacity of physically and chemically crosslinked cryogels, and cryogels produced by blending with cellulose crystals remains poorly described. There is a need to compare different types of crosslinking and blending agents, and characterize their effect on the mechanical properties of hydrogels and cryogels. Controlling the mechanical strength is important to develop performant superabsorbent when under load; lack of strength can lead to poor performance due to product disintegration.

The objective of this study is therefore to investigate, quantify and control the strength of nanocellulose hydrogels and cryogels. Carboxylated nanocellulose gels were produced that incorporated either: i) a chemical crosslinker (HMDA), ii) a physical crosslinker (PEI) or iii) cellulose crystal. The effect of chemical crosslinking, physical crosslinking, and dissimilar nanocellulose crystals addition on the structural, absorption, and strength properties of nanocellulose hydrogels and cryogels was compared. The structure of the different composites was analysed by Small Angle X-ray Scattering (SAXS) and related to the

properties of these gels for application as renewable, biocompatible and biodegradable superabsorbents. The developed superabsorbent has tuneable absorption and mechanical properties which make it suitable to remain integrated under load, such as for meat packaging or baby diaper.

2. Methodology

2.1. Materials

Bleached Eucalyptus Kraft (BEK) pulp, containing approximately 10 wt% solids, was obtained from Australian Paper, Maryvale, Australia. 2,2,6,6-Tetramethylpiperidine-1-oxyl (TEMPO), PEI (low molecular weight: M_w ~800 Da, M_n ~600 Da; high molecular weight: M_w ~ 750,000 Da, M_n ~ 60,000 Da), HMDA, MCC and sodium bromide (NaBr) were purchased from Sigma-Aldrich. CNC was purchased from The University of Maine, USA. Hydrochloric acid (HCl) and Sodium Hydroxide (NaOH) were diluted for solutions as required and were purchased from ACL Laboratories and Merck, respectively. 12 w/v% Sodium Hypochlorite (NaClO) was purchased from Thermo Fisher Scientific and used as received.

2.2. Solids concentration

The solids concentration of all samples (i.e. gel or pulp) was determined through oven drying. The sample was weighed before (w_i) and after (w_d) drying. Sample moisture was removed by drying in an oven (Thermoline BTC 9090) at 105 °C for at least 6 h. The solids content was calculated as:

$$Solid\ \ content\ (\%) = \frac{w_d}{w_i} \times 100\%$$

2.3. TEMPO mediated oxidation

The TEMPO-mediated oxidation of BEK pulp was done by using the oxidizing agent NaClO [10]. 25 g BEK pulp (dry weight) was suspended in 2500 mL water containing 0.4 g TEMPO and 2.5 g NaBr. The 12 w/v % NaClO solution was initially adjusted to pH 10 via addition of 36% HCl. To initiate the oxidation process, 100 mL NaClO was added drop-wise to the suspension whilst stirring. The pH of the reaction was monitored and maintained at 10 through the manual addition of 0.5 M NaOH. The oxidation process was completed in 3 h. The oxidized fibers were recovered through vacuum filtration and stored refrigerated (2–8 °C).

2.4. Conductometric titration

The carboxylate group content was measured by conductometric titration as reported in previous study [29]. Oxidized pulp samples (approx. 30 mg dry weight) were suspended in 40 mL deionized water. 200 μL of 1% NaCl was added to the suspended sample. The pH of the suspended sample was manually adjusted to between 2.5 and 3 with 0.5 M HCl prior to titration. Titration was accomplished by automated addition of 0.1 M NaOH using a Mettler Toledo T5 titrator. The conductivity of the sample was monitored throughout the titration progress. The carboxyl group content (mmol COO^-Na^+ /g fiber) was determined by:

$$CC = \frac{c\Delta V}{w} \times 1000$$

where ΔV pertain to the amount of titrant required to neutralize the carboxylic groups (in L), c is the NaOH concentration (mol/L), and w is the sample weight (g).

2.5. Physical crosslinking

TEMPO-oxidized pulp was dispersed in deionized water at the desired concentration (0.5 g dry fiber in 100 g suspension). Fibrillation was accomplished through a high-pressure homogenizer (GEA Niro Soavi Homogenizer Panda) at 1000 bar for two passes. One-pass homogenized gel was mixed with PEI using an electric hand mixer (ANCO 500). After thorough mixing, the gel was passed through the homogenizer for the second pass, after which physical crosslinking was assumed to have occurred. The samples were stored at 4 °C.

2.6. Chemical Crosslinking

Oxidized fiber was homogenised at the desired concentration (0.5 g dry fiber in 100 g suspension) at 1000 bar for two passes to produce nanocellulose gel. HMDA was dissolved in deionized water at a concentration of 0.45 g/mL. The nanocellulose gel was crosslinked with this HMDA in ratios of 2:1 and 1:1 (COO^-:NH_2) in presence of EDC/sulfo NHS. The gel was mixed for 5 mins and incubated at room temperature overnight (16 h).

2.7. Cellulose crystal blending

TEMPO-oxidized fiber suspension (0.5 g dry fiber in 100 g suspension) was blended with either MCC or CNC at a mass ratio of 2:1. After that fibrillation was achieved in the homogeniser at 1000 bar for two passes to produce the hydrogel.

2.8. Rheological measurement

Rheological testing of gel samples was performed with an Anton Paar MCR302 rheometer. A cone (0.997°) and plate (49.975 mm) geometry was selected. Testing was performed at ambient temperature (25 °C). A solvent trap was used to ensure stable temperature during measurements. Viscosity was measured at shear rates ranging from 0.5 to 100 s^{-1}. Oscillatory strain sweep was performed from 0.01% to 100% at a constant 1 Hz frequency.

2.9. Preparation of nanocellulose cryogels

The cryogels were prepared by spreading 12 g of gel evenly over the base of a 50 mm petri dish and freezing the sample at − 86 °C, then freeze-drying (Christ Alpha 2–4 LD Plus) for 2 days.

2.10. Fourier Transform Infrared (FTIR) spectroscopy

Cryogel samples were analysed by Fourier Transform Infrared (FTIR) spectroscopy (Agilent Technologies Cary 630 FTIR) which is equipped with a diamond attenuated total reflectance (ATR) accessory. Eight scans were taken at 4 cm^{-1} resolution.

2.11. Free swell capacity

The cryogel sample was placed in a glass funnel, which is immersed in a container full of testing fluid. To measure the absorption over time, the funnel with the sample was removed from the fluid container and the excess fluid allowed to drain for five minutes. The total mass was then measured at regular intervals of 3 h. The free swell capacity was then calculated as follows:

$$\text{Free Swell } Capacity(\text{FSC}) = \frac{m_t - m_i}{m_i}$$

Where m_t is the mass of the swollen cryogel at a particular time interval and m_i is the initial mass of the dry cryogel.

2.12. Compression testing

Cylindrical cryogel samples of 37 mm diameter and 37 mm length were prepared for compressive testing. Force-displacement data for cryogel samples was obtained by Instron model 5965 Universal Testing Machine equipped with 1 kN load cell. The testing was done at 23 °C and 50% humidity at a compression rare of 5 mm/min. The compressive Young's Modulus was determined from the slope of the initial linear region of the stress-strain curve.

2.13. SAXS

The SAXS measurements were conducted at the SAXS/WAXS beamline of the Australian Synchrotron. The wavelength was 1.03 Å and the measurements were conducted in the transmission mode.

3. Results

The structural and strength properties of physically (low molecular weight: LMW and high molecular weight: HMW PEI) and chemically (HMDA) crosslinked gels were quantified. Nanocellulose gel reinforced with cellulose fibrils of different length scales: long (MCC) and short (CNC) were also prepared and their properties compared with those of the crosslinked gels. The composition and identification of all nanocellulose gels are summarized in Table 1. The water content of physically crosslinked hydrogel and CNC blended hydrogel is compared with neat hydrogel in Table S1.

3.1. Physical crosslinked hydrogels

PEI was chosen as the physical crosslinker with nanocellulose hydrogel as it is known to adsorb on cellulose. The molecular weight of PEI plays an important role in determining the hydrogel strength. High molecular weight PEI improved the hydrogel strength significantly. Fig. 1 shows the rheological properties of hydrogels as a function of concentration for (a) low and (b) high molecular weight PEI. At low shear stress, the elastic modulus (G′) is dominant over the viscous modulus (G"), which indicates that the hydrogel behaves more like a solid material under these conditions, as G′ represents gel stiffness or strength. After the intersection point of G′ and G", the material flows like a liquid as the viscous modulus exceeds the elastic modulus. G" is the viscous or loss modulus; it indicates the portion of the deformation energy that is lost to internal friction during shearing. At first, G" is constant as the gel behaves like a uniform 3D network. G" then increases with increasing shear as micro cracks appear. Initially, the elastic behaviour is dominant. As shear increases further, micro cracks grow, merge and develop into continuous macro cracks which result in gel rupture at the highest value of G". Passed this point, the bulk material starts to flow, as indicated by the dominant viscous modulus (G") after the intersection of G′ and G", which occurs at the G" maxima.

Adding a low molecular weight PEI as a physical crosslinker weakens the nanocellulose hydrogel. Here, PEI acts a plasticizer and presents no evidence of crosslinking with cellulose. The viscous and elastic moduli of the LP adsorbed hydrogels (NC:LP) are lower than those of the nanocellulose hydrogel (Fig. 1a). The modulus intersections are also shifted toward higher shear strains, indicating a more cream-like behaviour of the hydrogel. The addition of 5 w/w % HP to nanocellulose hydrogels also does not significantly affect their rheological behaviour (Fig. 1b). However, increasing the HP concentration to 7 w/w % significantly increases the mechanical strength (by up to 5 times) compared to pure nanocellulose hydrogel (Fig. 1a) because of bridge formation between nanocellulose fibers. The intersection of G′ and G" also shifts to lower shear strain with increasing concentration of HP from 5 w/w % to 7 w/w %, indicating non-creamy or brittle hydrogel formation. The types of interaction between nanocellulose and PEI therefore depend on the molecular weight of PEI, which results in different hydrogel rheology.

Table 1
Description and characterization of the nanocellulose gels composition.

Sample code	Sample details
NC	Pure nanocellulose gel
NC:HP/ 1:0.05	Nanocellulose gel physically crosslinked with 5 w/w% HMW PEI
NC:HP/ 1:0.07	Nanocellulose gel physically crosslinked with 7 w/w% HMW PEI
NC:LP/ 1:0.05	Nanocellulose gel physically crosslinked with 5 w/w % LMW PEI
NC:LP/ 1:0.07	Nanocellulose gel physically crosslinked with 7 w/w% LMW PEI
NC:HMDA/ 2:1	Nanocellulose gel chemically crosslinked with HMDA at nanocellulose COO^- to amine ratio 2:1
NC:HMDA/ 1:1	Nanocellulose chemically crosslinked with HMDA with nanocellulose COO^- to amine ratio 1:1
NC:CNC/2:1	Nanocellulose blended with cellulose nano crystal at nanocellulose to CNC blend mass ratio 2:1
NC:MCC/2:1	Nanocellulose blended with MCC at nanocellulose to MCC blend mass ratio 2:1

3.2. Chemical crosslinked hydrogels

Chemical crosslinking of nanocellulose hydrogel with HMDA significantly increases hydrogel strength (Fig. 2). Adding HMDA to nanocellulose hydrogel at a carboxyl to amine group ratio of 2:1 results in a four-fold increase in the elastic modulus (G′) compared to the neat nanocellulose hydrogel. Increasing the HMDA ratio up to 1:1 augments G′ by 15 times. These increases in viscous and elastic moduli result from the formation of amide bonds between nanocellulose hydrogel carboxyl and the HMDA amine groups.

3.3. Blending cellulose fibrils to hydrogels

The strength of nanocellulose hydrogels blended with cellulose fibrils of different length scales - microscale with MCC or nanoscale with CNC - was tested (Fig. 3). These blended hydrogels do not show any significant change in G′ or G" compared to the neat nanocellulose hydrogel. However, blending the fibrils shifted the moduli intersections (shown by the vertical dotted lines in Fig. 3) to a lower shear strain of 10% for NC:CNC/2:1, 21.7% for NC:MCC/2:1 compared to neat NC at 31.7%, indicating the formation of a stronger gel.

3.4. Nanocellulose cryogels ATR-FTIR

Chemical crosslinking in the HMDA-NC cryogel was confirmed by ATR-FTIR (Fig. 4). The sharp peak at 1600 cm^{-1} for neat nanocellulose cryogel is due to the C═O stretching of the COO^- group on the oxidized fiber. For the crosslinked sample, C-N bending appears at 1240 cm^{-1} due to the presence of the amine group. C═O stretching from the amide bond is merged with the C═O stretching for COO^- group in the crosslinked sample. Fig. S3 shows all other samples FTIR spectra.

3.5. Cellulose cryogels mechanical strength

The compressive strength of the cryogels produced from the neat, crosslinked, and blended nanocellulose hydrogels is shown in Fig. 5. The cryogel produced from blended hydrogels showed increased mechanical strength. Neither chemical nor physical crosslinking of the hydrogels increased the mechanical strength of their cryogels. The stress-strain curve is shown in Fig. S4. Cryogel images at different states (before and after compression, after re absorption) are shown in Fig. S5.

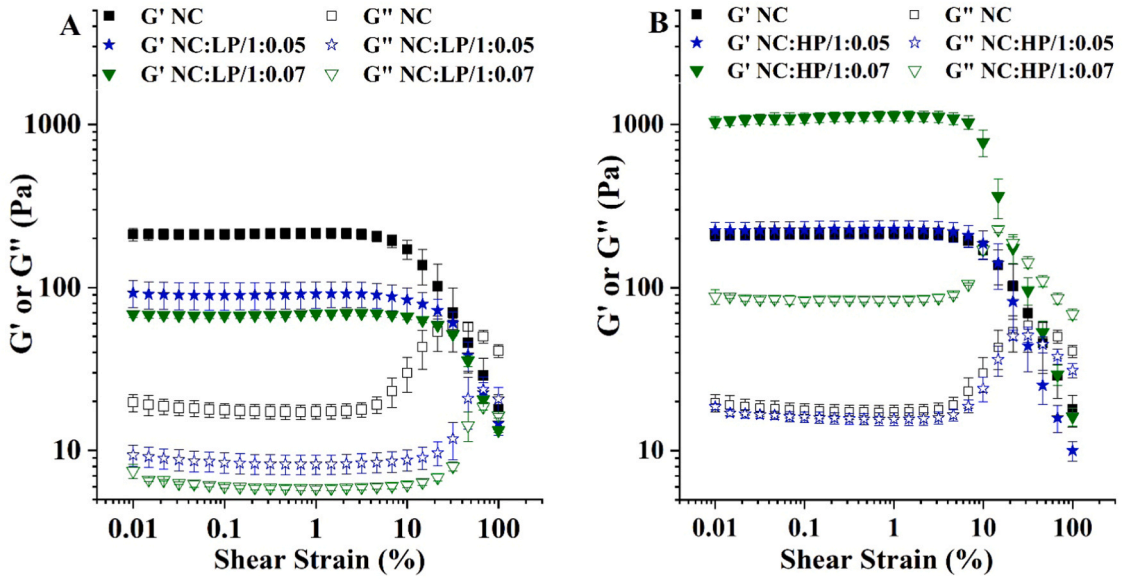

Fig. 1. Viscoelastic properties of TEMPO-oxidized cellulose hydrogels crosslinked with different concentrations of PEI varying in molecular weight: (A) hydrogels with low molecular weight PEI (LP) and (B) hydrogels with high molecular weight PEI (HP). Two PEI concentrations were tested: 5% and 7%, and the Elastic (G′) and viscous (G") moduli were recorded as a function of strain. Oscillation frequency and temperature were kept constant at 1 Hz and 25 °C, respectively.

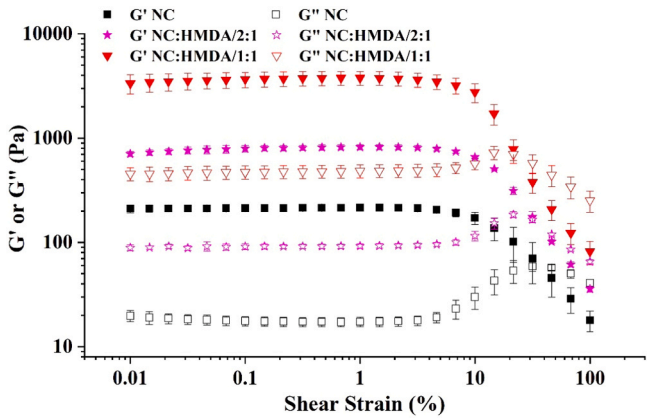

Fig. 2. Viscoelastic properties of TEMPO-oxidized cellulose hydrogels crosslinked with HMDA at different concentrations. Two NC:HMDA carboxyl to amine group ratio concentrations were tested: 1:1 and 2:1. Elastic (G′) and viscous (G") moduli were recorded as a function of strain. Measurements were performed at a frequency of 1 Hz and a temperature of 25 °C.

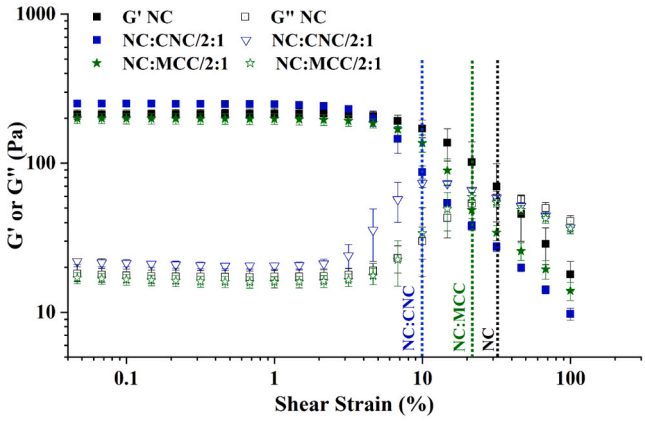

Fig. 3. Viscoelastic properties of TEMPO-oxidized cellulose hydrogels blended with CNC and MCC. NC:(CNC or MCC) ratio concentrations was set at 2:1. Elastic (G′) and viscous (G") moduli were recorded as a function of strain. Measurements were performed at a frequency of 1 Hz and a temperature of 25 °C. The moduli intersection points are indicated by the vertical dotted lines.

3.6. Nanocellulose cryogel Free swell capacity

The free swell capacity (FSC) and water retention capacity (WRC) of the neat nanocellulose cryogel are the highest (Fig. 6). The physically and chemically crosslinked cryogels have the lowest absorption and water retention capacity, while the cryogels blended with CNC and MCC show intermediate performance. Physically and chemically crosslinked cryogels showed a decrease in free swell capacity of 48% and 51% respectively, compared to the neat nanocellulose cryogel.

3.7. Structural analysis by Small Angle X-ray Scattering (SAXS)

SAXS measurements were performed to reveal the network structure and fiber arrangement, and to visualize the water penetrating the spaces in hydrogel, cryogel and rewetted cryogel samples (Fig. 7). The different sections of the SAXS curve reveal the fiber structural arrangement at different dimensions before and after water penetration.

For hydrogels, the SAXS curves for neat and crosslinked samples show significant differences, indicating variations in structure (Fig. 7a). The upturn in the lower q value (0.003–0.006 $Å^{-1}$) of all curves indicates that the surface scattering from the large structures of bigger pores/interfibrillar spaces is similar. However, there is noticeable difference in the SAXS curve shape observed between $q = 0.003$ and 0.2 $Å^{-1}$. The bump in this range is due to the difference in scattering length between the water and the cellulose fibers. The neat nanocellulose hydrogel curve shows a bump between $q = 0.015$ and 0.22 $Å^{-1}$, corresponding to a pore size range of 42–2.8 nm. The HMDA crosslinked hydrogel shows large bump area between $q = 0.01$ and 0.23 $Å^{-1}$, indicating a larger pore size range of 63–2.7 nm. The HP crosslinked hydrogel shows a bump similar to that of HMDA; however, the bump is more pronounced in the HMDA-crosslinked sample. This indicates that both crosslinked samples have large open structures, but that the HMDA crosslinked sample has a more homogenous distribution of spaces than the HP crosslinked sample. The CNC blended hydrogel shows a shift in

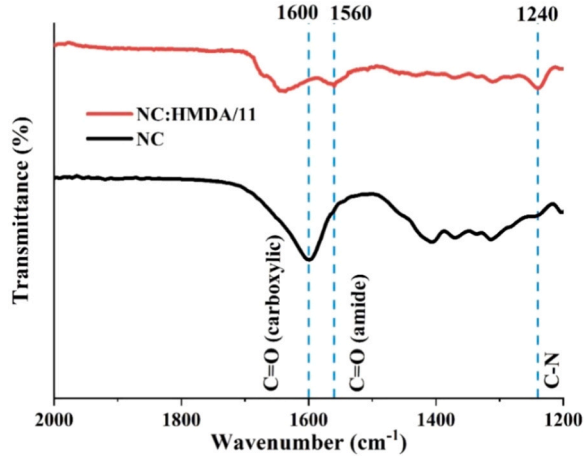

Fig. 4. ATR-FTIR spectra of pure nanocellulose cryogel and chemically (HDMA) crosslinked cryogel demonstrating effective chemical reaction.

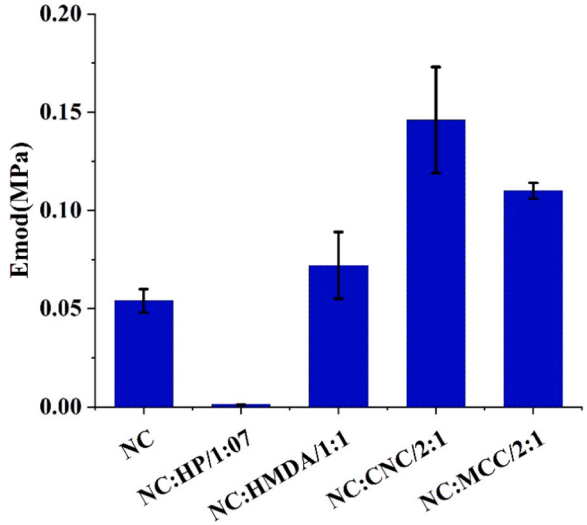

Fig. 5. Effect of crosslinking and blending on the compressive modulus (E_{mod}) of nanocellulose cryogels.

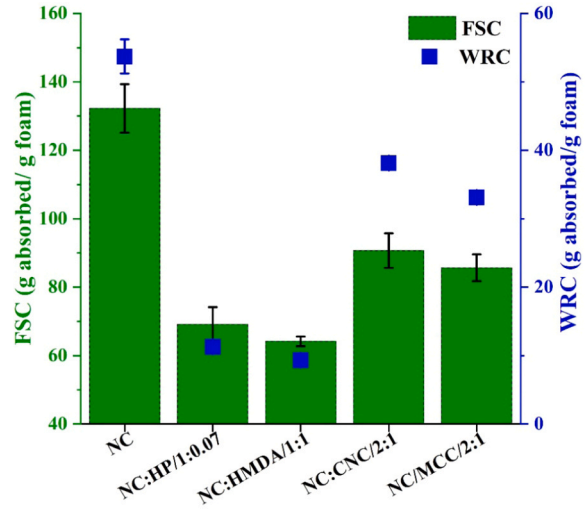

Fig. 6. Free swell capacity (FSC) and water retention capacity (WRC) of nanocellulose cryogels tested for MilliQ water.

the bump towards a q range of between 0.002 and 0.06 $Å^{-1}$, corresponding to a pore size range of 314–11 nm. The large size range in the blended sample is due to the repulsion between the cellulose fibers and CNC which forces the network to expand and creates more space between fibers.

For the cryogels, the SAXS curves do not show any significant difference among samples, except for HMDA crosslinked cryogel (Fig. 7b). The curves follow the power law of q^{-4}, indicating that the cellulose fibers tend to aggregate during drying, and therefore leave large size structures and open-air spaces in the resulting cryogels. However, the HMDA crosslinked sample shows a bump ($q = 0.05–0.2$ $Å^{-1}$), indicating the presence of some smaller size pores of size ranging between 12 and 2 nm in the structure.

Upon rewetting, water is absorbed into both the fibers and the pores of the cryogels. The SAXS curves from rewetted cryogels (Fig. 7c) show significant differences compared to the dried samples (Fig. 7b). The bumps in the rewetted sample curves indicate that the scattering from the swollen fibres and the spaces between them are filled with water. In all samples, the bump appears at almost the same q range (0.014–0.22 $Å^{-1}$). The corresponding pore size range of the space is between 45 and 2.8 nm. This indicates the water molecules penetrate and occupy similar sized spaces between fibers in all samples. However, the fiber bundle swelling behavior is significantly different between the samples, as reported previously for PEI and HMDA crosslinked samples [24]. At the low q range (< 0.014 $Å^{-1}$) the power law ranges from $q^{-3.5}$ to q^{-4}, indicating that the larger structure is formed by fiber entanglement and large pores.

The SAXS curves of the rewetted cryogels also differ from their corresponding hydrogels. This qualitatively indicates that the presence and correlation of the water molecules with the network is different in the hydrogels and rewetted cryogels. Therefore, simply rewetting a cryogel does not reform the corresponding hydrogel due to differences in the fiber structure of the hydrogels and cryogels that lead to differences in the interactions of the water molecules with and within the structure upon rewetting.

4. Discussion

4.1. Effect of crosslinking and blending on nanocellulose hydrogels

TEMPO oxidized nanocellulose hydrogels are made of entangled nanocellulose fibrils held together by electrostatic stabilization [50]. Here, chemical or physical crosslinkers and cellulose fibrils are used to modify the properties of the hydrogels. Physical crosslinking of nanocellulose hydrogel with a dendrimer polyelectrolyte such as PEI affects the rheological properties (to higher or lower elastic moduli) depending on the polymer molecular weight. Chemical crosslinking with HMDA increases the elastic moduli of the gel because of strong amide bond formation between the negative carboxylic group of cellulose and the positive amine of HMDA. Blending nano or micro cellulose fibrils does not have any significant effect on the elastic or viscous moduli of the hydrogel.

PEI molecular weight plays an important role in the hydrogel rheology. For the low molecular weight polyelectrolytes of high charge density, neutralization of the nanocellulose fiber charge occurs by the positively charged PEI amine group [51,52] (Fig. 8A), decreasing inter-fiber repulsion between the COO^- groups. The LP molecule is too short to link COO^- groups and form a bridge between nanocellulose fibers and therefore acts as a plasticizer, increasing the liquid-like behavior of the hydrogel. This is indicated by the low G′ and G” measured for LP crosslinked hydrogel (Fig. 1A) [53]. Conversely, bridging between the PEI amine groups and nanocellulose fiber COO^- groups does occur for HP [54,55] (Fig. 8b), as revealed by the increase of G′ and G” by up to 5 times for HP crosslinked hydrogel over the neat nanocellulose hydrogel.

Chemical crosslinking with HMDA produces a strong chemical bond,

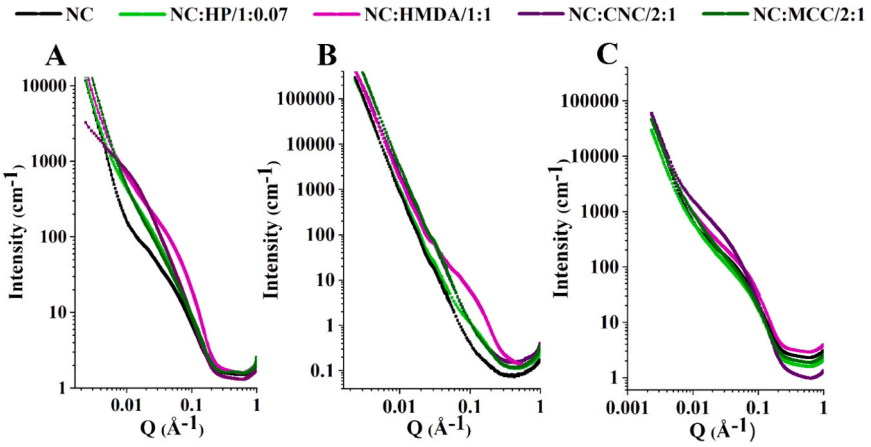

Fig. 7. Small Angle X-ray (SAXS) measurements of (A) Hydrogel, (B) Cryogel and (C) cryogel rewetted with MilliQ water.

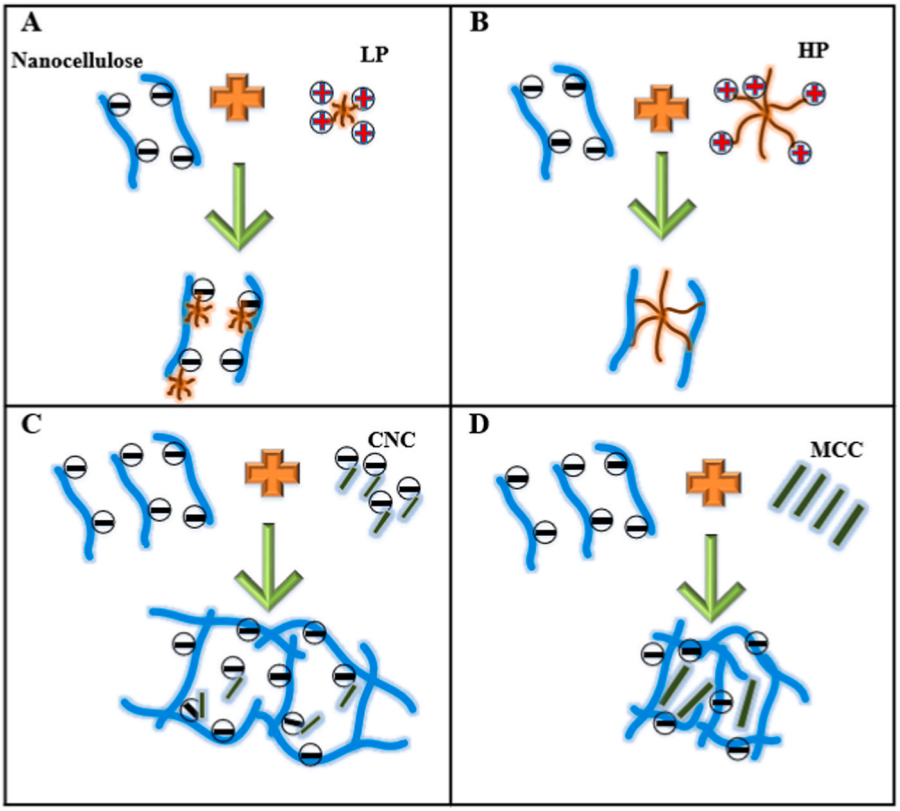

Fig. 8. Schematic representation of the crosslinking interaction and blending agents with nanocellulose (A) nanocellulose with LP, (B) nanocellulose with HP, (C) nanocellulose with CNC and (D) nanocellulose with MCC.

resulting in higher elastic and viscous moduli for the chemically crosslinked hydrogel than for the physically crosslinked hydrogel. The strong crosslinking density of the HMDA sample was 1.40 mol/m^3, and HP crosslinked hydrogel has a lower crosslinking density of 0.44 mol/m^3.

CNC has a strong negative surface charge which repels the negative charge of oxidized nanocellulose fibers (Fig. 8C). MCC particles have no specific surface charge, resulting in gels with a heterogeneous structure, as indicated by the SAXs curve (Figs. 7A and 8D). As a result, the blended hydrogel with CNC has a much more homogeneous structure compared to the blended MCC hydrogel, as revealed by a hump in SAXS scattering for CNC blended hydrogel (Fig. 7A). However, the rheological properties of MCC and CNC blended hydrogels are not significantly different to those of the neat hydrogel. This is because they do not form fiber-fiber bonds, unlike those created in crosslinked hydrogels.

4.2. *Effect of crosslinking and blending on nanocellulose cryogels*

Nanocellulose hydrogels are freeze dried into cryogels. Crosslinking or blending a nanocellulose hydrogel prior to drying affects the mechanical and absorption properties of the resulting cryogel differently depending on the crosslinking or blending type and density. In this study, the mechanical properties of cryogels were quantified by compressive strength and their absorption capacities measured by free swell capacity measurements followed by centrifugation to determine the water retention capacity.

The HP crosslinked cryogel structure is very open compared to the

original nanocellulose one, as revealed by SAXs analysis (Fig. 7). Structural openness is also visible in these samples via optical microscopy and SEM imaging, as shown in Fig. S1 and S2. The HP crosslinked cryogel shows the lowest compressive strength due to its more open and brittle structure [24]. The compressive strength of the chemically crosslinked (HMDA) cryogel does not change significantly, compared to the neat sample, as the small HMDA molecules only crosslink between adjacent fibers, which does not increase the compressive modulus of the corresponding cryogel. Blended CNC hydrogels result in corresponding cryogels with a significantly increased compressive strength of 0.146 MPa compared to 0.054 MPa for the neat nanocellulose cryogel. CNC has a much smaller particle diameter (~5 nm) than MCC (~50 μm). The surface area of reinforcement provided by CNC is four orders of magnitude higher than for MCC, resulting in a higher area of interaction, increased structural reinforcement, and therefore the highest mechanical strength results for CNC-NC blended cryogel.

The neat nanocellulose cryogel shows the highest absorption capacity, while chemically and physically crosslinked cryogels have similar, lower absorption capacity, despite their significant structural differences. The compact structure of the chemically crosslinked hydrogel, which is a result of the amide-COO^- bond formation, hinders water penetration within the pores of the material, resulting in a lower absorption capacity than the neat cryogel. The open structure of the physically crosslinked cryogel cannot contain as much water, therefore also resulting in lower absorption capacity [24] and water retention capacity than that of the neat cryogel. For cryogels made by blending MCC or CNC, the absorption properties decrease in comparison to those of the neat sample because of the lower availability of COO^- groups and the incorporation of cellulose crystals, which hinder water penetration inside the structure (Fig. 6).

Physical and chemical crosslinking with HP and HMDA, respectively, does increase the mechanical strength of the resulting hydrogel, but not that of the corresponding cryogel. The CNC blended NC cryogel shows increased compressive strength due to the higher area of reinforcement resulting from the incorporation of the small, rod shaped, negatively charged CNC particles. So, although hydrogels and cryogels are simply different forms of a nanocellulose gel having the same original chemical composition, their mechanical strengths vary significantly as a function of crosslinking and blending.

5. Conclusion

A family of cellulose hydrogels and cryogels was developed from TEMPO oxidized cellulose nanofibers (CNF) by incorporating physical and chemical crosslinkers or by blending with cellulose fibrils of different relative lengths. The effect of the type of crosslinking or cellulose crystal addition on the mechanical properties of both the hydrogel and corresponding cryogel was quantified. Gel properties were measured by rheology, mechanical strength, and absorption capacity; structure was quantified by SAXS, optical and scanning electron microscopy. Differences in the properties were related to differences in the hydrogel and cryogel composition, structure and mechanical strength.

Chemically crosslinked hydrogel showed the highest strength compared to all other hydrogel because of strong chemical bond between nanocellulose and the crosslinker. Hydrogels physically crosslinked with high molecular weight PEI had higher elastic and viscous moduli than neat nanocellulose hydrogel due to fiber bridging. Crosslinking with a low molecular weight PEI reverses the behavior, showing decreased elastic and viscous moduli due to charge neutralization. This highlights the effect of PEI molecular weight on the strength of oxidized cellulose nanofiber gels. The addition of CNC or MCC to CNF to create a blended hydrogel had no significant effect on the rheological properties.

The highest cryogel compressive strength was achieved by blending CNC with CNF. Chemical crosslinking with HMDA did not affect the cryogel compressive strength significantly. However, physical crosslinking with high molecular weight PEI significantly decreased the compressive strength of the nanocellulose cryogel by opening up its structure. The neat nanocellulose cryogel has the highest free swell capacity and water retention capacity as it has the highest concentration of available COO^- groups.

This study quantifies the effect of chemical and physical crosslinking and cellulose crystal blending on the structure and mechanical properties of NC hydrogels and cryogels. These results improve the understanding of the hydrogel-cryogel structure-property relationships and facilitate the development of tunable hydrogel and cryogel materials for food, agriculture and diagnostic applications.

CRediT authorship contribution statement

Laila Hossain: Conceptualization, Visualization, Methodology, Investigation, Software, Writing – original draft. **Vikram Singh Raghuwanshi:** Software, Writing – review & editing. **Joanne Tanner:** Supervision, Writing – review & editing. **Gil Garnier:** Visualization, Supervision, Writing – review & editing.

Declaration of Competing Interest

The authors declare that they have no known competing financial interests or personal relationships that could have appeared to influence the work reported in this paper.

Acknowledgements

Financial support was received from Meat and Livestock Australia (grant number P.PSH. 0890). The authors acknowledge Australian Synchrotron for the facilities used. Thanks to Assoc Professor Rico Tabor for the rheological facilities. The authors also acknowledge Mahdi Naseri-Nosar to provide help with the optical microscope.

Appendix A. Supporting information

Supplementary data associated with this article can be found in the online version at doi:10.1016/j.colsurfa.2021.127608.

References

[1] S. Kiatkamjornwong, Superabsorbent polymers and superabsorbent polymer composites, Sci. Asia 33 (1) (2007) 39–43.
[2] M.J. Zohuriaan-Mehr, K. Kabiri, Superabsorbent polymer materials: a review, Iran. Polym. J. 17 (6) (2008) 451.
[3] F. Masuda, Trends in the Development of Superabsorbent Polymers for Diapers, ACS Symp. Ser. (1994) 88–98.
[4] E. Caló, V.V. Khutoryanskiy, Biomedical applications of hydrogels: a review of patents and commercial products, Eur. Polym. J. 65 (2015) 252–267.
[5] J. Li, D.J. Mooney, Designing hydrogels for controlled drug delivery, Nat. Rev. Mater. 1 (12) (2016) 1–17.
[6] J. Li, A. Celiz, J. Yang, Q. Yang, I. Wamala, W. Whyte, B. Seo, N. Vasilyev, J. Vlassak, Z. Suo, Tough adhesives for diverse wet surfaces, Science 357 (6349) (2017) 378–381.
[7] J.D. Tang, C. Mura, K.J. Lampe, Stimuli-responsive, pentapeptide, nanofiber hydrogel for tissue engineering, J. Am. Chem. Soc. 141 (12) (2019) 4886–4899.
[8] C. García-González, M. Alnaief, I. Smirnova, Polysaccharide-based aerogels—promising biodegradable carriers for drug delivery systems, Carbohydr. Polym. 86 (4) (2011) 1425–1438.
[9] B. Zavan, R. Cortivo, G. Abatangelo, Hydrogels and tissue engineering. Hydrogels, Springer,, 2009, pp. 1–8.
[10] R.M. Barajas-Ledesma, A.F. Patti, V.N. Wong, V.S. Raghuwanshi, G. Garnier, Engineering nanocellulose superabsorbent structure by controlling the drying rate, Colloids Surf. A: Physicochem. Eng. Asp. 600 (2020), 124943.
[11] X. Cui, J.J. Lee, W.N. Chen, Eco-friendly and biodegradable cellulose hydrogels produced from low cost okara: towards non-toxic flexible electronics, Sci. Rep. 9 (1) (2019) 1–9.
[12] G. Tang, B. Zhou, F. Li, W. Wang, Y. Liu, X. Wang, C. Liu, X. Ye, Advances of Naturally Derived and Synthetic Hydrogels for Intervertebral Disk Regeneration, Front. Bioeng. Biotechnol. 8 (2020) 745.
[13] A. Sannino, C. Demitri, M. Madaghiele, Biodegradable cellulose-based hydrogels: design and applications, Materials 2 (2) (2009) 353–373.
[14] R.M. Barajas-Ledesma, L. Hossain, V.N. Wong, A.F. Patti, G. Garnier, Effect of the counter-ion on nanocellulose hydrogels and their superabsorbent structure and properties, J. Colloid Interface Sci. 599 (2021) 140–148.

[15] A. Vazquez, M.L. Foresti, J.I. Moran, V.P. Cyras, Extraction and production of cellulose nanofibers. Handbook of Polymer Nanocomposites. Processing, Performance and Application, Springer,, 2015, pp. 81–118.
[16] D. Trache, M.H. Hussin, C.T.H. Chuin, S. Sabar, M.N. Fazita, O.F. Taiwo, T. Hassan, M.M. Haafiz, Microcrystalline cellulose: isolation, characterization and bio-composites application—a review, Int. J. Biol. Macromol. 93 (2016) 789–804.
[17] Y. Chen, X. Jiang, H. Wu, L. Zheng, Bi-directional tuning of thermal transport in SrCoOx with electrochemically induced phase transitions, Nat. Mater. 19 (03) (2020) 655–662.
[18] Y. Habibi, H. Chanzy, M.R. Vignon, TEMPO-mediated surface oxidation of cellulose whiskers, Cellulose 13 (6) (2006) 679–687.
[19] T. Abitbol, A. Rivkin, Y. Cao, Y. Nevo, E. Abraham, T. Ben-Shalom, S. Lapidot, O. Shoseyov, Nanocellulose, a tiny fiber with huge applications, Curr. Opin. Biotechnol. 39 (2016) 76–88.
[20] S. Ahmed, S. Ikram, Chitosan based scaffolds and their applications in wound healing, Achiev. Life Sci. 10 (2016) 27–37.
[21] O.A.T. Dias, S. Konar, A.L. Leão, W. Yang, J. Tjong, M. Sain, Current state of applications of nanocellulose in flexible energy and electronic devices, Front. Chem. 8 (2020) 420.
[22] H. Chavda, C. Patel, Effect of crosslinker concentration on characteristics of superporous hydrogel, Int. J. Pharm. Investig. 1 (1) (2011) 17–21.
[23] S. Sinha, Biodegradable superabsorbents: methods of preparation and application—a review. Fundamental Biomaterials: Polymers, Woodhead Publishing,, 2018, pp. 307–322.
[24] L. Hossain, V.S. Raghuwanshi, J. Tanner, C.-M. Wu, O. Kleinerman, Y. Cohen, G. Garnier, Structure and swelling of cross-linked nanocellulose foams, J. Colloid Interface Sci. 568 (2020) 234–244.
[25] G.T. Hermanson. Bioconjugate Techniques, Academic press,, 2013.
[26] N. Kayra, A.Ö. Aytekin, Synthesis of cellulose-based hydrogels: preparation, formation, mixture, and modification, Cellul. -Based Superabsorbent Hydrogels (2019) 407–434.
[27] F. Jiang, Y.-l Hsieh, Super water absorbing and shape memory nanocellulose aerogels from TEMPO-oxidized cellulose nanofibrils via cyclic freezingthawing, J. Mater. Chem. A 2 (2) (2013) 350–359.
[28] L. Liu, L. Bai, A. Tripathi, J. Yu, Z. Wang, M. Borghei, Y. Fan, O.J. Rojas, High axial ratio nanochitins for ultrastrong and shape-recoverable hydrogels and cryogels via ice templating, ACS Nano 13 (3) (2019) 2927–2935.
[29] S.H. Zainal, N.H. h Mohd, N. Suhaili, F.H. Anuar, A.M. Lazim, R. Othaman, Preparation of cellulose-based hydrogel: a review, J. Mater. Res. Technol. (2020).
[30] X. Zhang, W. Huo, S. Yan, Y. Chen, K. Gan, J. Liu, J. Yang, Innovative application of PVA hydrogel for the forming of porous Si3N4 ceramics via freeze-thaw technique, Ceram. Int. 44 (11) (2018) 13409–13413.
[31] Y. Guan, J. Bian, F. Peng, X.-M. Zhang, R.-C. Sun, High strength of hemicelluloses based hydrogels by freeze/thaw technique, Carbohydr. Polym. 101 (2014) 272–280.
[32] H. Zhang, F. Zhang, J. Wu, Physically crosslinked hydrogels from polysaccharides prepared by freeze–thaw technique, React. Funct. Polym. 73 (7) (2013) 923–928.
[33] S. Butylina, S. Geng, K. Oksman, Properties of as-prepared and freeze-dried hydrogels made from poly (vinyl alcohol) and cellulose nanocrystals using freeze-thaw technique, Eur. Polym. J. 81 (2016) 386–396.
[34] S. Butylina, S. Geng, K. Laatikainen, K. Oksman, Cellulose nanocomposite hydrogels: from formulation to material properties, Front. Chem. 8 (2020) 655.
[35] S.F. Kabir, P.P. Sikdar, B. Haque, M.R. Bhuiyan, A. Ali, M. Islam, Cellulose-based hydrogel materials: chemistry, properties and their prospective applications, Prog. Biomater. 7 (3) (2018) 153–174.
[36] K. Syverud, H. Kirsebom, S. Hajizadeh, G. Chinga-Carrasco, Cross-linking cellulose nanofibrils for potential elastic cryo-structured gels, Nanoscale Res. Lett. 6 (1) (2011) 1–6.
[37] W. Hu, Z. Wang, Y. Xiao, S. Zhang, J. Wang, Advances in crosslinking strategies of biomedical hydrogels, Biomater. Sci. 7 (3) (2019) 843–855.
[38] M.E. El-Naggar, S.I. Othman, A.A. Allam, O.M. Morsy, Synthesis, drying process and medical application of polysaccharide-based aerogels, Int. J. Biol. Macromol. 145 (2020) 1115–1128.
[39] H. Zhuo, Y. Hu, Z. Chen, L. Zhong, Cellulose carbon aerogel/PPy composites for high-performance supercapacitor, Carbohydr. Polym. 215 (2019) 322–329.
[40] T. Budtova, Cellulose II aerogels: a review, Cellulose 26 (1) (2019) 81–121.
[41] J. Patiño-Masó, F. Serra-Parareda, Q. Tarrés, P. Mutjé, F.X. Espinach, M. Delgado-Aguilar, TEMPO-oxidized cellulose nanofibers: a potential bio-based superabsorbent for diaper production, Nanomaterials 9 (9) (2019) 1271.
[42] P.C. Thapliyal, K. Singh, Aerogels as promising thermal insulating materials: an overview, J. Mater. 2014 (10) (2014) 1–10.
[43] Z. Ulker, C. Erkey, An emerging platform for drug delivery: aerogel based systems, J. Control. Release 177 (2014) 51–63.
[44] M.N. Alam, L. Christopher, Natural cellulose-chitosan crosslinked superabsorbent hydrogels with superior swelling properties, ACS Sustain. Chem. Eng. 6 (7) (2018) 8736–8742.
[45] D.J. Mendoza, L. Hossain, C. Browne, V.S. Raghuwanshi, G.P. Simon, G. Garnier, Controlling the transparency and rheology of nanocellulose gels with the extent of carboxylation, Carbohydr. Polym. 245 (2020), 116566.
[46] R.M. Barajas, V. Wong, K. Little, A.F. Patti, G. Garnier, *Carboxylated Nanocellulose Superabsorbent: Biodegradation and Soil Water Retention Properties*, J. Appl. Polym. Sci. (2021) 51495.
[47] E.M. Ahmed, Hydrogel: preparation, characterization, and applications: a review, J. Adv. Res. 6 (2) (2015) 105–121.
[48] T. Zhang, Y. Zhang, X. Wang, S. Liu, Y. Yao, Characterization of the nano-cellulose aerogel from mixing CNF and CNC with different ratio, Mater. Lett. 229 (2018) 103–106.
[49] D. Burhani, A.A. Septevani, R. Setiawan, L.M. Djannah, M.A. Putra, S.S. Kusumah, D. Sondari, Self-assembled behavior of ultralightweight aerogel from a mixture of CNC/CNF from oil palm empty fruit bunches, Polymers 13 (16) (2021) 2649.
[50] R. Curvello, V.S. Raghuwanshi, G. Garnier, Engineering nanocellulose hydrogels for biomedical applications, Adv. Colloid Interface Sci. 267 (2019) 47–61.
[51] J. Gregory, Rates of flocculation of latex particles by cationic polymers, J. Colloid Interface Sci. 42 (2) (1973) 448–456.
[52] Y. Adachi, L. Feng, M. Kobayashi, Kinetics of flocculation of polystyrene latex particles in the mixing flow induced with high charge density polycation near the isoelectric point, Colloids Surf. A: Physicochem. Eng. Asp. 471 (2015) 38–44.
[53] J. Gregory, S. Barany, Adsorption and flocculation by polymers and polymer mixtures, Adv. Colloid Interface Sci. 169 (1) (2011) 1–12.
[54] T.K. Wang, R. Audebert, Flocculation mechanisms of a silica suspension by some weakly cationic polyelectrolytes, J. Colloid Interface Sci. 119 (2) (1987) 459–465.
[55] Y. Zhou, G.V. Franks, Flocculation mechanism induced by cationic polymers investigated by light scattering, Langmuir 22 (16) (2006) 6775–6786.